

# Analysis of branon dark matter and extra-dimensional models with AMS-02

Jose A. R. Cembranos<sup>\*,1</sup>, Álvaro de la Cruz-Dombriz<sup>†,2</sup>, Peter K. S. Dunsby<sup>‡,2,3</sup> and Miguel Méndez-Isla<sup>§2</sup>

<sup>1</sup>*Departamento de Física Teórica I and UPARCOS,  
Universidad Complutense de Madrid, E-28040 Madrid, Spain*

<sup>2</sup>*Cosmology and Gravity Group, Department of Mathematics and Applied Mathematics,  
University of Cape Town, Rondebosch 7701, Cape Town, South Africa.*

<sup>3</sup>*South African Astronomical Observatory, Observatory 7925, Cape Town, South Africa*

In the following work, we compute the positron production from branon dark matter annihilations in order to constrain extra-dimensional theories. By having assumed that the positron fraction measured by AMS-02 is well explained just with astrophysical sources, exclusion diagrams for the branon mass and the tension of the brane, the two parameters characterising the branon phenomenology become possible. Our analysis has been performed for a minimal and a medium diffusion model in one extra dimension for both pseudo-isothermal and Navarro-Frenck-White dark matter haloes. Our constraints in the dark matter mass candidate range between 200 GeV and 100 TeV. Combined with previous cosmological analyses and experimental data in colliders, it allows us to set bounds on the parameter space of branons. In particular, we have discarded regions in the mass-tension diagram up to a branon mass of 28 TeV for the pseudo-isothermal profile and minimal diffusion, and 63 TeV for the Navarro-Frenck-White profile and medium diffusion.

PACS numbers: 04.50.Kd, 98.80.-k, 98.80.Cq, 12.60.-i

## I. INTRODUCTION

The bump reported above 8 GeV of the positron fluxes at the International Space Station (ISS) by some detectors such as AMS-02 [1–3], PAMELA [4, 5] HEAT [6] or Fermi [7], has opened a wide discussion about the origin and the reliability of models of cosmic-ray propagation. This bump has been usually considered as an expected excess added to a modeled background to which other astrophysical sources are added [8, 9]. The main astrophysical candidates to interpret such a result are supernovae remnants [10], the secondary production of positrons in the interstellar medium (ISM) generated by spallation of cosmic rays [11] and nearby pulsars [12]. Hence, taking into account the contributions from averaged distant sources, fluxes from both local supernovae (Green Catalog [13]) and pulsars from the ATNF [14] (such as Geminga, J1741-2054 or Monogem), the measurements of AMS-02 can be well fitted [8].

Complementarily, there is a general agreement on the fact that one part (when not the whole) of the excess could be attributed to more exotic sources, such as dark matter (DM) [15–18]. Even if the AMS-02 data can be just explained with astrophysical sources, it is not possible to omit that an outstanding variety of astrophysical and cosmological phenomena require an explanation in terms of DM. Among these observations, the most remarkable evidence are, among others, the case of DM in the Coma [19, 20] and Bullet Clusters [21, 22], the

flat galactic rotation curves [23, 24], gravitational lensing [25], Nucleosynthesis abundances, the anisotropies in the Cosmic Microwave Background (CMB) and the growth of large structures [26]. From these different evidences, some properties of DM can be inferred: namely, it was non-relativistic matter at the moment of decoupling [27], it is stable or long-lived [28], effectively non-photon-interacting [29], collisionless [30], dissipationless [31], smoothly distributed at cosmological scales [32] and sufficiently heavy [33].

From the particle physics point of view, as well as supported by the thermal decoupling, one of the best candidate for DM are the so-called Weakly Interactive Massive Particles (WIMPs). Several DM models have been proposed (*c.f.* [34, 35] and references therein) in order to explain the WIMPs features which cannot be accommodated within the Standard Model of elementary particles. In this paper, we shall focus on the so-called extra-dimensional brane-world theories [36–41], where a 4-dimensional brane is embedded in a  $D$ -dimensional bulk ( $D > 4$ ). As a result of the brane fluctuations in the bulk, it is possible to define a pseudo-scalar Nambu-Goldstone boson, dubbed branon, which emerges due to an explicit translational symmetry breaking [40–47]. Moreover, branon fields can be shown to be massive, stable and weakly interacting, which makes them a competitive candidate for WIMPs which can naturally accommodate the correct amount and properties of DM particles. Although branons are prevented from decaying into SM particles by parity invariance on the brane, they may still annihilate by pairs into different channels of the SM. These products after the annihilation could decay or hadronise resulting in stable particles such as electrons/positrons, protons/antiprotons, neutrinos, gamma rays [48] or antimatter [49].

On the other hand, as suggested by galactic rotation

\*cembra [at] fis.ucm.es

†alvaro.delacruzdombriz [at] uct.ac.za

‡peter.dunsby [at] uct.ac.za

§mndmig001 [at] myuct.ac.za

curves, the DM disposition in halos in which galaxies are immersed causes that DM particles annihilate at the so-called point of the injection (in the halo) and its stable products can propagate along the galaxy through a convoluted transport process. Such a propagation may cause signals to be detected at the Earth directly in form of annihilation products or in secondary processes of these stable particles with the galactic environment, such as radio signals of synchrotron radiation [50–53] or gamma rays in the case of Inverse Compton Scattering. As such, these signatures could be potentially measured by different detectors conforming the so-called DM indirect searches [15–18]. In this manuscript we shall focus our interest on positron flux. Indeed, taking into account the amount of sources that can explain the positron excess, we shall follow a cautious method in order to constrain the range of masses, the tension and - therefore the thermal averaged cross section - of the branons to explain AMS-02 results [1–3]. Thus, our analysis will address whether it is necessary to include pulsars, supernovae remnants (SNRs) and DM contributions in order to explain the AMS-02 excess or whether the DM signal is negligible and consequently not detectable within some statistical significance. In both cases it is possible to constrain the range of masses, the tension and therefore the cross section of the branons.

Let us highlight at this stage that eventual detection of indirect signals would not constitute a conclusive evidence for DM since the uncertainties in the model-dependent DM interactions, DM density distribution in the halo and backgrounds from other astrophysical sources still remain entangled and not fully understood yet. With this caveat in mind, this work precisely focuses on the possibility of the indirect detection method to get information about the DM nature, abundance and properties using positron signals. Such an analysis obviously needs to be combined with other indirect detection searches using photons, neutrinos, electrons, protons, antiprotons or antimatter [54] that can be observed in detectors like Fermi-LAT [55], IceCube or Antares [56].

The paper is organised as follows: in Sec. II, we shall describe the propagation of positrons when obtained from the DM annihilation in our galaxy, the importance of each term in the transport equation governing the propagation, and how the latter can be treated as a mere diffusion equation in the case of positrons. In addition, we shall discuss about the source term that contains information about the DM model encapsulated in the thermal averaged cross section, DM mass and its astrophysical disposition in halos. Then, in Sec. III, in order to illustrate our line of reasoning, we shall move from the Particle-Physics Model-Independent approach to specify the underlying theory of WIMPs in the form of branons. Next, in Sec. IV we shall summarise the technicalities emerging in the solution for the diffusion equation in terms of Bessel-Fourier series. Such a solution will allow us to describe, in Sec. V, the signature generated for the

extra-dimensional branons in the positron fraction over a specified model of background and therefore herein, we shall provide our constraints for the branon parameter space when combined with other previous analyses. Finally, Sec. VI shall be devoted to the main conclusions of the work.

## II. TRANSPORT OF COSMIC RAYS AND THE positron/electron CASE

### A. Generalities

Cosmic rays are immersed in an environment governed by turbulent galactic magnetic field. The departing point to describe the problem is by use of a combination of the continuity equation with the Fick's law [57] as follows

$$\frac{\partial n}{\partial t} - D_{xx} \nabla \cdot (\nabla n) = Q(\mathbf{r}, t). \quad (1)$$

The continuity equation takes into account the conservation of number of particles inside a volume and the latter explains that the current of particles  $\mathbf{j}$  is proportional to the concentration variation through  $\mathbf{j} = -D_{xx} \nabla n$ , where  $n$  is the number density of particles and  $D_{xx}$  represents the diffusion coefficient. This coefficient is in principle a tensor [58], that depends on the energy of the cosmic rays and whose elements describe the diffusion when cosmic rays travel parallel or perpendicular to the magnetic field. It is therefore a diffusion description that takes into account the behaviour of the particles with the magnetic field.

On the other hand,  $Q(\mathbf{r}, t)$  holds for the source term which describes the injection of the cosmic rays, in our case due to the DM annihilation. Using Eq. (1) as a first approximation of the problem it is then possible to add therein different mechanisms in the transport of cosmic rays along the galaxy [59] so the result is the so-called Ginzburg-Syrovatsky equation for the number density of particles per unit of energy  $\psi = n/E$  [60, 61],

$$\begin{aligned} \frac{\partial \psi}{\partial t} = & \nabla \cdot (D_{xx} \nabla \psi - \mathbf{V} \psi) + \frac{\partial}{\partial p} D_{pp} \frac{\partial}{\partial p} \frac{1}{p^2} \psi \\ & - \frac{\partial}{\partial p} [b(p) \psi - (p/3)(\nabla \cdot \mathbf{V})] - \frac{1}{\tau_f} \psi - \frac{1}{\tau_r} \psi + Q(\mathbf{r}, p, t); \end{aligned} \quad (2)$$

where  $p$  is the total momentum of the particle at position  $\mathbf{r}$ . The main contributions on the right-hand side of Eq. (2) can be summarised as follows: The first additional term is characterized by the tensor  $D_{pp}$  and can be understood as a diffusive process in the momentum space, the so-called reacceleration term [62, 63], which considers the probability of having multiple accelerations of cosmic-ray particles in the interaction with the magnetohydrodynamic (MHD) shock wave in the interstellar medium (ISM).

Secondly, another mechanism that could be relevant in the transport of cosmic rays is the convection associated to the galactic wind  $\mathbf{V}$  because of the stellar activity in late stellar stages that could push the ISM and the magnetic field out of the galactic plane being the net effect an outflow perpendicular to the galactic plane. In addition, this mechanism not only implies a density redistribution but also a term of adiabatic losses  $-\frac{p}{3}(\nabla \cdot \mathbf{V})$  in the expansion of the plasma [64].

Then, the term in Eq. (2) referred to radiative losses [65, 66] is proportional to the loss of energy rate per unit of time  $b(p)$ . This might be of great importance for some cosmic-ray species, not only because its relevance in the dynamic of cosmic rays along the galaxy (this term for instance suppresses cosmic rays at very high energies), but it could also be responsible for new signatures to be detected. In fact the signal production due to the synchrotron emission or the Inverse Compton Scattering is taken into account in this term. The main mechanisms in the loss of energy included in  $b(p)$ , range from Coulombian interactions, bremsstrahlung, synchrotron emission to Inverse Compton Scattering. Eq. (5) below will provide further details for such contributions.

Finally, coming back to Eq. (2) the strike of primary cosmic rays, i.e., those coming directly from the source, with ISM particles may produce secondary cosmic rays in a process dubbed spallation through fragmentation or radioactive decay of the particles being  $\tau_f$  and  $\tau_r$  the time scale for each case respectively.

Now that we have thoroughly described the terms in (2), we can simplify its form by assuming the validity of a quasi-linear theory regime, in which there is a magnetic field with short fluctuations ( $\delta B \ll B$ ), the diffusion tensor turns out to be a scalar  $D_{xx} \sim D(R)$ , where  $R = pc/Ze$  is the rigidity that gives the answer of a particle under a magnetic field. Under those circumstances, the most conventional diffusion model renders  $D(R) = K_0 \left(\frac{p}{mc}\right)^\delta (R/\text{GV})^\delta$  with the rigidity  $R$  measured in gigavolts. As we can see, the diffusion coefficient is dependent on the energy and can be parametrized by two constants  $K_0$  and  $\delta$ .

Moreover, under this approximation the space diffusion coefficient  $D_{xx}$  and the reacceleration parameter  $D_{pp}$  are correlated by [62, 67];

$$D_{xx}D_{pp} = p^2 V_A^2 \frac{1}{\delta(4-\delta)(4-\delta^2)}, \quad (3)$$

where  $V_A \sim 20$  km/s is the Alfvén velocity of the MHD wave. In the case of positrons, since they travel with velocities close to the speed of light, the diffusion term is one of the most relevant terms. The reacceleration parameter  $D_{pp}$  is inversely proportional to the diffusion one according to Eq. (3). If the latter is dominant the probability of having a second acceleration can be neglected.

On the other hand, the convection velocity takes values of  $|\mathbf{V}| \sim 10$  km/s [68] which is negligible with respect to the relativistic velocity of the positrons. In addition, in this study we shall only calculate the contribution of positrons due to the DM annihilation without considering the spallation terms  $-\frac{1}{\tau_f}\psi - \frac{1}{\tau_r}\psi$  in Eq. (2) since this mechanism will be taken as a part of a background model to be analysed in Sec. V. Once a steady-state has been reached, it is possible to obtain a purely diffusion equation for positrons from Eq. (2) yielding

$$-K_0 \epsilon^\delta \nabla^2 \psi - \frac{\partial}{\partial E}(b(E)\psi) = Q(\mathbf{r}, E) \quad (4)$$

where  $b(E)$  is the radiative losses term in the energy space which can be split in the following contributions [65]

$$b(E) = b_{\text{brem}}(E) + b_{\text{coul}}(E) + b_{\text{ISRF}}(E) + b_{\text{syn}}(E), \quad (5)$$

where  $b_{\text{brem}}(E)$  includes the deflection of cosmic rays by atoms and molecules of the ISM,  $b_{\text{coul}}(E)$  describes the interaction among cosmic rays and charged particles of the thermal plasma of the background,  $b_{\text{ISRF}}(E)$  describes the Inverse Compton Scattering of the interstellar Radiation Field (ISRF) in which photons came from different sources, increasing its frequency due to the scattering with relativistic electrons of the medium such as the CMB, star radiation and infrared radiation emitted by interstellar dust. Finally, the synchrotron radiation due to the cosmic rays accelerated by the galactic magnetic field can be described by  $b_{\text{syn}}(E)$ . Thus, in Table I we have provided analytical expressions for each term in Eq. (5).

Radiative losses contributions	
$b_{\text{brem}}(E) \simeq 1.51 \cdot 10^{-16} n_e \gamma [\ln(\gamma) + 0.36]$	
$b_{\text{coul}}(E) \simeq 1.2 \cdot 10^{-12} n_e \left[ 1 + \frac{\ln(\frac{\gamma}{n_e})}{75} \right]$	
$b_{\text{ISRF}}(E) = \frac{4}{3} \frac{\sigma_T}{m_e c} \gamma^2 U_{\text{rad}}$	
$b_{\text{syn}}(E) = \frac{4}{3} \frac{\sigma_T}{m_e c} \gamma^2 U_B$	

Table I: Analytical expressions for each term in Eq. (5).  $n_e$  is the number density of electrons in the plasma and  $\gamma$  is the Lorentz factor,  $U_{\text{rad}} = 0.9$  eV/cm<sup>3</sup> is the energy density of radiation (starlight, emission from dust and CMB),  $\sigma_T$  is the Thomson cross section,  $m_e$  is the electron mass,  $c$  is the speed of light. and  $U_B = \frac{B^2}{8\pi}$  is the magnetic energy density in cgs.

As seen in Fig. 1, at high energies, the form in which electrons/positrons lose energy is mainly through Inverse Compton Scattering and synchrotron emission. Consequently, both  $b_{\text{coul}}(E)$  and  $b_{\text{brem}}(E)$  can be neglected in Eq. (4).

The advantage of constraining DM through cosmic rays lies in the fact that other signals caused by different processes summarised in Table I becomes possible. Thus these losses range from radio emission frequencies found in processes involving synchrotron losses to gamma rays

of the Inverse Compton scattering. The using of multiple tests could show some confrontations allowing us to rule out some models [69].

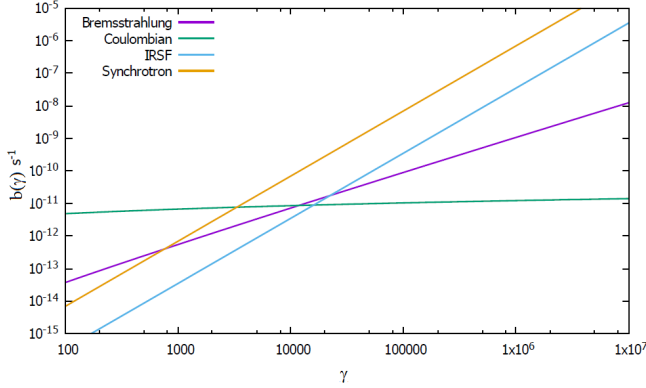


Figure 1: Radiative losses at different energies for positrons plotted against  $\gamma = E/m_e c^2$ . Synchrotron emission due to the acceleration by the galactic magnetic field (assumed in the figure as  $6 \mu\text{G}$ ) and Inverse Compton Scattering of low energy photons are the most relevant terms whenever electrons/positrons are ultra-relativistic.

As mentioned above, the source term in Eq. (4),  $Q(\mathbf{r}, E)$  includes information of the source injecting positrons in the environment [70, 71]. Provided the only source of positrons is the DM annihilation, then

$$Q(\mathbf{r}, E) = \frac{1}{2} \langle \sigma v \rangle \left( \frac{\rho(\mathbf{r})}{M_{\text{DM}}} \right)^2 \sum_j \beta_j \frac{dN_e^j}{dE}, \quad (6)$$

where  $\langle \sigma v \rangle$  is the total thermal averaged cross section of annihilation,  $\rho(\mathbf{r})$  is the DM density profile of the halo,  $M_{\text{DM}}$  is the DM mass,  $\frac{dN_e^j}{dE}$  is the injection spectra of the positron due to DM annihilation at the annihilation point and  $\beta_j = \frac{\langle \sigma v_j \rangle}{\langle \sigma v \rangle}$  the branching ratio that provides the annihilation probability in one particular channel  $j$ . Both the injection spectra and the thermal averaged cross section are DM model-dependent quantities, the latter to be analysed in the Sec. III.

On the other hand, it is necessary to describe how DM is disposed in haloes through DM density profile  $\rho(\mathbf{r})$ . As seen in Fig. 2, the DM profiles agree at long distances from the centre. However, significative differences can be seen for radii smaller than 8 kpc (in Fig. 2 we use the parametrization of the halos from the reference [49]). In the following we shall use the pseudo-isothermal DM halo

$$\rho_{\text{ISO}}(r) = \frac{\rho_0 r_a^2}{(r^2 + r_a^2)}, \quad (7)$$

(with  $r_a = 5 \text{ kpc}$  and  $\rho_0 = 1.53 \text{ GeV cm}^{-3}$ ) and the Navarro-Frenck-White (NFW):

$$\rho_{\text{NFW}}(r) = \frac{\rho_s}{\frac{r}{r_s} \left( 1 + \frac{r}{r_s} \right)^2}, \quad (8)$$

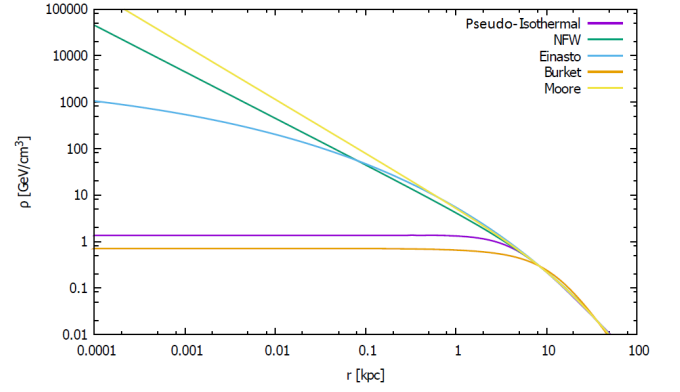


Figure 2: Several dark matter halo profiles in the Milky Way using halos parameterisation as given in Ref. [49]. The Milky Way radius has been taken as  $R_g = 20 \text{ kpc}$ . All the profiles are similar in the outer regions. NFW, Einasto and Moores profile are classified as cuspy models and despite of the fact they are supported by DM simulations, experimental data points towards a more cored profile such as the Burkert profile. This correction can be related with the presence of baryons that are relevant in inner regions. The pseudo-isothermal profile requires the halo to be in a steady state.

where  $\rho_s$  is the scale density and it is defined by  $\rho_s = \frac{3H(z)^2 \delta_c}{8\pi G}$  that contains information about the Universe at the moment that the halo collapsed. As we can see, there is a discontinuity at  $r = 0$  and the NFW DM profile density tends to infinity. This singularity needs to be regularized in order to find finite results. Indeed, we have worked with a modified NFW model to simulate the core at the centre of the galaxy according to the study of [15], so

$$\rho_{\text{NFW}}^*(r) = \rho_{\text{NFW}}(r_0) \left[ 1 + 8.11 \cdot \text{sinc} \left( \frac{\pi r}{r_0} \right) + 6.11 \cdot \text{sinc} \left( \frac{2\pi r}{r_0} \right) \right]^{1/2}, \quad (9)$$

which is valid for  $r < r_0$ , whereas for  $r > r_0$ , expression (8) for the standard NFW DM profile remains valid. Thus, the  $r_0$  value represents the overlapping radius between both functions (8) and (9). It is important to set off that it is possible to smooth the NFW profile without changing the physics of the problem since for values of  $r_0 \approx 10^{-7} \text{ pc}$ , we can ensure that solutions of the diffusion equation (4) do not vary significantly at  $r < r_0$ .

### III. BRANONS AS WIMPS CANDIDATES

Some extra-dimensional theories understand our universe to be a 4-dimensional space-time embedded in a  $D$ -dimensional bulk being the extra dimensions compactified extra dimensions, this is the so-called brane-world scenario. In this theoretical frame, Standard Model (SM) particles are confined in a spatial 3-brane and only



the gravitational interaction propagates in the bulk of the space-time. The fluctuations of the brane can be parametrized by branon fields, which from the point of view of an observer within the brane, are new particles. [54, 72–85]. Indeed, branons are pseudo-scalar fields,  $\pi^\alpha$ , which can be understood as Pseudo-Goldstone bosons because of the breaking of the translational symmetry in the bulk space produced by the presence of the brane. Branons can be weakly interacting, stable and massive what makes them good candidates for DM. Thus, in the frame of low energy-effective Lagrangian theories, the interaction of branons with SM particles yields [86–90, 92, 93]

$$\mathcal{L}_{Br} = \frac{1}{2}g^{\mu\nu}\partial_\mu\pi^\alpha\partial_\nu\pi^\alpha - \frac{1}{2}M^2\pi^\alpha\pi^\alpha + \frac{1}{8f^4}(4\partial_\mu\pi^\alpha\partial_\nu\pi^\alpha - M^2\pi^\alpha\pi^\alpha g_{\mu\nu})T^{\mu\nu}, \quad (10)$$

with  $\alpha = 1 \dots \mathcal{N}$ , with  $\mathcal{N}$  the number of branon species. As seen in Eq. (10), branons couple through the stress-energy tensor  $T^{\mu\nu}$  with an interaction suppressed by the brane tension  $f^4$ . On the other hand, the parity invariance of the brane prevents them from decaying into SM particles.

On the other hand, the parity invariance of the brane prevents them from decaying into SM particles.

For branons, the annihilation cross sections depend solely upon the branon mass, and the mass and spin of the SM particle. The thermal average annihilations are represented in Fig 3, where one can find the  $\langle\sigma_i v\rangle$  expressions in all the allowed SM particles channels, i.e., in fermions, vector gauge bosons and scalars. [82, 94]. Below we provide the leading term for non-relativistic branons. For the annihilation into a Dirac fermion  $\psi$  with mass  $m_\psi$ , the cross section becomes

$$\langle\sigma_\psi v\rangle = \frac{1}{16\pi^2 f^8} M^2 m_\psi^2 (M^2 - m_\psi^2) \sqrt{1 - \frac{m_\psi^2}{M^2}}. \quad (11)$$

For a massive gauge field  $Z$ , of mass  $m_Z$ , it reads:

$$\langle\sigma_Z v\rangle = \frac{1}{64\pi^2 f^8} M^2 (4M^4 - 4M^2 m_Z^2 + 3m_Z^4) \times \sqrt{1 - \frac{m_Z^2}{M^2}}, \quad (12)$$

whereas for a massless gauge field  $\gamma$ , the leading order is zero

$$\langle\sigma_\gamma v\rangle = 0, \quad (13)$$

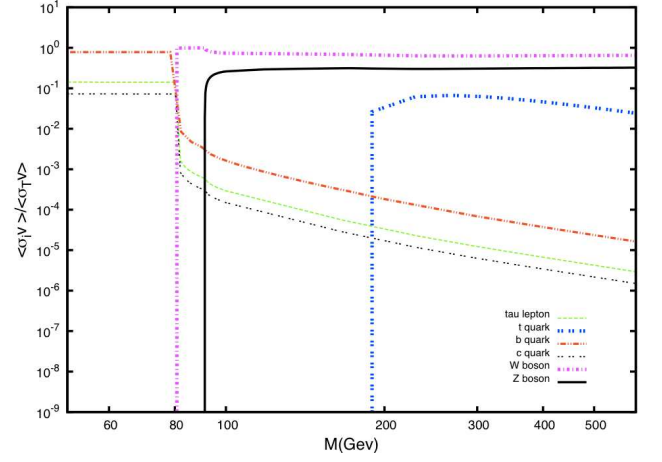


Figure 3: Annihilation branching ratios for extra-dimensional branons in different channels as taken from [91]. The annihilation into leptons is highly suppressed excepting for lighter branons (until a mass of  $\sim 80$  GeV), although the annihilation is mainly via  $b\bar{b}$ . From this mass, other kinds of processes are opened, in which the annihilation is mostly via  $Z^+Z^-$  and  $W^+W^-$ . Our work is centered in this latter range of masses.

and, finally, for a (complex) scalar field  $\Phi$  of mass  $m_\Phi$ :

$$\langle\sigma_\Phi v\rangle = \frac{1}{32\pi^2 f^8} M^2 (2M^2 + m_\Phi^2)^2 \sqrt{1 - \frac{m_\Phi^2}{M^2}}. \quad (14)$$

Finally, monochromatic gamma-ray line is also expected at the energy equal to the branon mass as a consequence of direct annihilation into photons since branons couple directly to them. However, this annihilation takes place in  $d$ -wave channel and consequently it is highly suppressed.

Restrictions and prospects on the model parameters from tree-level processes have been obtained for colliders such as ILC, LHC or CLIC [92, 93, 95–97]. Also, further astrophysical and cosmological bounds were obtained in [54, 72–85].

The possibility of the annihilation of branons opens a window to detect them by discriminating different signatures. As we mentioned before, they could annihilate producing SM particles, which may decay or hadronise into cosmic rays. Hence, positrons that branons can inject to the environment are related to  $\sum_j \beta_j \frac{dN_e^j}{dE}$  appearing in Eq. (6). In Fig. 4 we observe that the amount of positrons increases with the mass of the branon so positrons are mainly generated at high energies after branons annihilation. However, it is not expected to see positrons at very high energies after the propagation since the losses of energy are more pronounced at this range. Our analysis about the injection spectra of branon has used the functions  $\frac{dN_e^j}{dE}$  taken from PPC4DMID [98, 99] for every annihilation channel  $j$ .

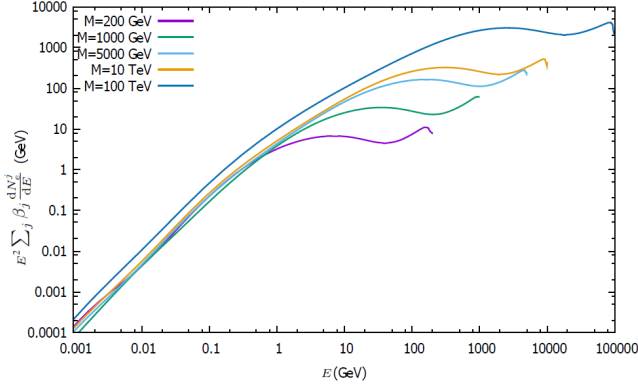


Figure 4: The spectra of positron at the point of injection at the galactic environment (before the propagation). The tension of the brane is not relevant in the represented quantity since the branching ratio is independent of it. As it is possible to see, the annihilation produces positrons mostly at high energies. In order to compute the total injection spectra we use the functions from PPC4DMID [98, 99].

#### IV. FLUXES AT THE EARTH

The transport diffusion zone for positrons in our galaxy is modeled as a cylinder of radius  $R_g$  and thickness  $2L_z$  centered at the center of the galaxy. At the coordinates  $R_g$  and  $L_z$ , it is considered that the density of electrons/positrons is negligible with regard to the rest of the density in the galaxy, so that the boundary conditions to solve the Equation (3) are  $\psi(R_g, z) = 0$  and  $\psi(r, \pm L_z) = 0$ . The solution of the Eq. (2) can be expressed in terms of Bessel-Fourier series [15, 49] as follows,

$$\psi(\vec{x}, E) = \sum_{i=1}^{\infty} \sum_{n=0}^{\infty} J_0\left(\frac{\alpha_{0,i}}{R}r\right) \varphi_b(z) P_{i,n}(E), \quad (15)$$

where  $J_0$  are Bessel functions of first kind with  $\alpha_{0,i}$  zeros and  $\varphi_b(z) = \sin\left(\frac{n\pi}{2L}(z + L_z)\right)$ . In our results we have checked that the relative error adding the  $(n+1)^{th}$  or  $(i+1)^{th}$  term does not exceed more than 0.1% with respect to the truncation at  $n^{th}$  and  $i^{th}$  terms in the sum above. In the case of Isothermal profile with MIN diffusion we have taken around  $i, n \simeq 15$  terms whereas for NFW with MED diffusion it was necessary around  $i \approx 60$  and  $n \approx 20$  terms to get the required precision. On the other hand, the dependence of the density  $\psi$  with the energy is given by

$$P_{i,n}(E) = \frac{1}{b(E)} \int_E^{M_{DM}} dE_s Q_{i,n}(E_s) \cdot \exp\left(-\frac{\lambda_D^2(E, E_s)}{4} \left\{ \left(\frac{n\pi}{2L_z}\right)^2 + \left(\frac{\alpha_i^2}{R^2}\right) \right\}\right). \quad (16)$$

The solution of electron/positron density is a particular case of a more general solution based on the Green's

method. In this method the cosmic-ray particles are generated at position  $x_s$  and time  $t_s$  with an energy  $E_s$ . Once the particles are injected at the source, they reach the coordinates  $(x, t)$  with an energy  $E$ . The distance between these two points is called the diffusion length  $\lambda_D$ , which satisfies

$$\lambda_D^2(E, E_s) = 4 \int_E^{E_s} d\varepsilon \frac{K_0 \varepsilon^\delta}{b(\varepsilon)}. \quad (17)$$

Finally the factor  $Q_{i,n}(E_s)$  in Eq. (16) corresponds to the Bessel and Fourier transforms of the source term as follows

$$Q_{i,n}(E_s) = \frac{2}{L_z R^2 J_1^2(\alpha_i)} \times \int_0^R \int_{-L_z}^{L_z} r dr dz J_0\left(\frac{\alpha_{0,i}}{R}r\right) \varphi_b(z) Q(\mathbf{r}, E_s). \quad (18)$$

By considering that the Solar System is about  $r \simeq 8$  kpc and  $z \simeq 0$ , we can obtain the fluxes of electrons/positrons at the Earth as purely generated by DM annihilation, i.e., without considering any background from standard astrophysical sources. Hence the positron flux at the Earth becomes

$$\Phi_{e^\pm}^{DM}(\mathbf{r}_\odot, E) = \frac{v_e(E)}{4\pi c} \psi(\mathbf{r}_\odot, E), \quad (19)$$

where  $v_e$  is the electron/positron velocity which in a general case depends on the energy  $E$ . In our case we consider ultra-relativistic electrons/positrons, i.e.,  $v_e(E) \simeq c$ . In Fig. 5, it is possible to observe that after the propagation, the cosmic rays energy maximum does not happen at high energies, as we observed in the point of injection (see Fig. 4). In the case of the branons with a tension of  $f = 200$  GeV the maximum of  $E$  is 1% of the highest energy and in the case of  $f = 100$  GeV around a  $10^{-5}\%$ . In addition, Fig. 5 also shows how higher tensions  $f$  of the brane lowers the received flux for positrons.

#### V. BACKGROUND MODEL AND COMPARISON WITH AMS02 RESULTS

The comparison with the experimental results of AMS-02 has been done using the positron fraction from the CRDB database of charged cosmic rays [100] where the data for the quantity

$$\mathcal{F}_{e^+} = \frac{\Phi_{e^+}(E)}{\Phi_{e^+}(E) + \Phi_{e^-}(E)} \quad (20)$$

are provided. The conundrum of a correct description for the positron fraction not only lies in the explanation of it either with a DM model or with one (or several) astrophysical sources, but also in fitting it with a correct

combination of all the aforementioned contributions. Even if it is possible to fit the positron fraction only with astrophysical sources, it could be possible taking into account that the DM contribution seems not to produce a visible signature over the background.

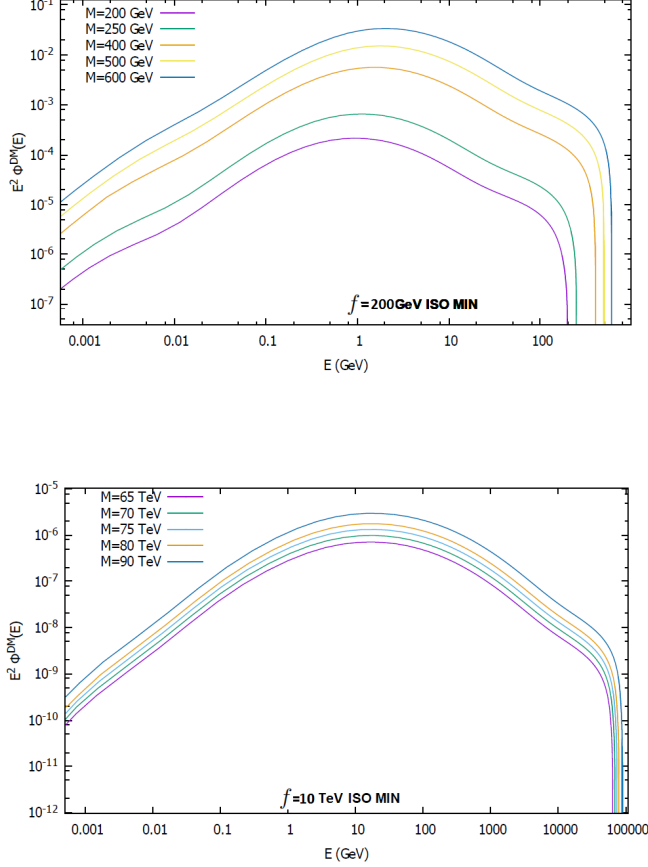


Figure 5: Flux of positrons at the Earth after the propagation, for a minimal diffusion (MIN) of a pseudo-isothermal profile and constant magnetic field equal to  $6 \mu\text{G}$  for different tensions of the brane. The top panel corresponds to  $M = 200$  GeV and the bottom panel corresponds to  $M = 10^4$  GeV. The characteristic cut off of the annihilation signature at the mass of the branon can be observed in the panels.

In our analysis we shall follow the reasoning that since it is possible to fit the AMS-02 data set with an astrophysical background, the DM contribution to the positron fraction (20) would be negligible when compared with the background. Hence, according to the model in [101, 102], let us divide the non-modulated (NM) positron flux  $\Phi_{e^+}^{\text{NM}}$  in its primary and secondary components of cosmic rays  $\Phi_{e^+}^{\text{NM}}(E) = \Phi_{e^+}^{\text{prim}}(E) + \Phi_{e^+}^{\text{sec}}(E) + \Phi^{\text{DM}}(E)$ , with

$$\begin{aligned}\Phi_{e^+}^{\text{prim}}(E) &= C_s E^{-\gamma_s} \exp(-E/E_s), \\ \Phi_{e^+}^{\text{sec}}(E) &= C_{e^+} E^{-\gamma_{e^+}}\end{aligned}\quad (21)$$

where both  $\Phi_{e^+}^{\text{prim}}$  and  $\Phi_{e^+}^{\text{sec}}$  refer to background contributions.

Primary astrophysical sources for positrons can be produced in a pulsar environment under strong magnetic fields through the decay of high-energy photons into positron-electron pairs. Secondary ones are produced because of the collision of the primary component with the ISM in the process of spallation. On the other hand, although it is not relevant in the range of energies of the excess, in principle a correction should be considered because of the solar modulation at low energies. Consequently, and following the force field approximation:

$$\Phi_{e^+}(E) = \frac{E^2}{(E + \phi_{e^+})^2} \Phi_{e^+}^{\text{NM}}(E + \phi_{e^+}). \quad (22)$$

In the case of electrons, the flux caused by nearby SNRs and pulsars, can be well fitted through a combination of two power laws<sup>1</sup> as follows

$$\Phi_{e^-}(E) = \frac{E^2}{(E + \phi_{e^-})^2} [C_1 (E + \phi_{e^-})^{\gamma_1} + C_2 (E + \phi_{e^-})^{\gamma_2}]. \quad (23)$$

Taking into account the expressions of this section, we have calculated the positron fraction for the  $(f, M_{\text{DM}})$  parameter space of parameters describing DM particles originated in brane-world scenarios. For illustrative purposes, we have considered one extra dimension in a range of masses between 200 GeV and 100 TeV. In this range of masses, branons mainly annihilate via  $Z^+Z^-$  and  $W^+W^-$  as seen in Fig. 3. These bosons will then generate positrons. We have firstly performed our calculations for a minimal model of propagation (MIN) of an pseudo-isothermal profile and secondly, for a medium propagation (MED) of a NFW profile. The magnetic field taken was constant and fixed to  $B = 6 \mu\text{G}$ .

In Fig. 6 we observe that the positron fraction increases with  $M$  due to the fact that the cross section of annihilation presented in (12) also increases with  $M$  enhancing the source term  $Q(\mathbf{r}, E)$  (6). Then, the dependence of the cross section with  $M$  compensates the inverse square suppression of  $Q(\mathbf{r}, E)$ . Previous literature has usually considered the thermal averaged cross section,  $\langle\sigma v\rangle$  as a constant. This will result in that the source term for the annihilating dark matter turns out to be inversely proportional to the WIMP mass. Consequently the positron fraction would decrease with the mass. Notwithstanding, in the case of branons the cross section scales as  $M^6$  for massive gauge fields

<sup>1</sup> The parameters of the fluxes  $C_s, \gamma_s, E_s, C_{e^+}, \gamma_{e^+}, \phi_{e^+}, C_{e^-}, \gamma_{e^-}, \phi_{e^-}, \gamma_1, \gamma_2$  can be obtained from [18]. Such values are suitable for a range of energies between 2 and 350 GeV.

so the signal of positrons increases with the branon mass.

In addition, the effect of the brane tension is suppressing the probability of interaction between DM particles (12), so that, it is possible to observe in Fig. 7 a decreasing of the positron fraction with  $f$ . However, the effect of mass can compensate the suppression of the tension for low values ( $f, M$ ). It means that for a tension of  $f = 200$  GeV the masses that can give a measurable increasing of the positron fraction are around  $M = 200$  GeV. However, as the tension gets bigger the bump of positron fraction is not visible even for very high masses. For instance, for a tension of  $f = 10$  TeV massive branons with  $M = 50$  TeV would not generate any signature.

## VI. CONCLUSIONS

In this work we have set constraints on the parameter space for brane-world theories using the AMS-02 positron excess. In order to do so, we have assumed the signal can be fully explained, within the error bars and statistical significance by different astrophysical sources so the eventual dark matter contribution will be negligible. Since brane-world theories provide natural candidates for dark matter particles, we have generated exclusion diagrams for the space  $(f, M)$  being  $f$  the brane tension and  $M$  the mass of the dark matter particle identified with the brane oscillations, dubbed branon, which satisfies standard WIMPs properties. Figure 7 encapsulates such exclusion diagrams for one extra dimension. In order to determine excluded regions in the  $(f, M)$  space we have used a likelihood analysis at the 95% confidence level. Although we know that  $\chi^2$  test is not strictly well used, since the error bars do not strictly follow a Gaussian distribution. Thus, strictly speaking, it would necessary to perform variations in the whole space of both astrophysical and dark-matter model parameters in order to get the statistical significance of the predictions. Nonetheless, up to the level of accuracy we seek, our approximation suffices to put constraints on branons features.

Our analysis has shown that the Navarro-Frank-White model with medium diffusion is more restrictive than the Isothermal with minimal diffusion as we can see in Fig. 7. The former involves more amount of DM at the centre of the galaxy and a longer diffusion length  $\lambda_D$ , so that, a bigger fraction of products than that expected in the Isothermal model with minimal diffusion would reach the Earth. On the other hand, Eq. (6) shows that the fluxes of positrons from branons (annihilating in all the channels) can be computed as a linear superposition of the flux of every channel separately (i.e: instead of solving the equation one time with all the channels together  $\sum_j \beta_j \frac{dN_j}{dE}$  solving the diffusion equation for every channel. Taking into account that the tension is a multiplicative factor in (6) for every channel, we could extract it and taking it as a decreasing boost factor. It would be possible to include then, the usual boost factor due

to the clumps of DM in the halo by defining an effective tension. Considering that the multiplicative factor in Eq. (12) and hence in Eq. (6) is inverse to the eight power of the tension scale re-absorption of the boost factor  $B$  it is not very significant.

Following [103], we combine the exclusion area from AMS-02 with previous works in the diagram  $(f, M)$ . The model MED, NFW is more restrictive than MIN, ISO as we can see in Fig. 7. The former involve more amount of DM at the center of the galaxy and a greater  $\lambda_D$ , so that, a bigger fraction of products than expected in MIN, ISO would reach the Earth. The limit in which the description of the effective theory branons is valid is also represented in Fig. 7 that will be the upper limit in the range of masses for our study.

In Fig. 8 we present a map of exclusion for branons combining the results of this work with previous studies ([103]). As we observe, DM models computed in this work does not reach the blue solid line. It means that it is not able to rule out the thermal region where branons acquire the dark matter abundance by the standard freeze-out mechanism. As we have commented, the addition of boost factor could slightly modify the parameter space constraints plotted in Fig. 8.

Finally, let us mention that this is not the only study that one can do with the AMS-02 measurements. Indeed, both the total flux for electrons and positrons have been measured separately with AMS-02 and the separate analysis of every flux might constrain indirect DM signals as well [69]. However, as described in the bulk of our study, we have found a high sensitivity of the positron fraction with the brane tension, so that it has not been necessary considering other experimental results to get competitive constraints in the branon parameters space.

## Acknowledgments

The authors would like to thank Carlos Muñoz Lopez from IFT/CSIC-UAM and Roy Maartens from UWC for useful comments. JARC and AdlCD acknowledge financial support from the projects FIS2016-78859-P European Regional Development Fund and Spanish Research Agency (AEI), FIS2014-52837-P (Spanish MINECO) and Consolider-Ingenio MULTIDARK CSD2009-00064. AdlCD also acknowledges financial support from projects FPA2014-53375-C2-1-P Spanish Ministry of Economy and Science, CA15117 CANTATA and CA16104 COST Actions EU Framework Programme Horizon 2020, CSIC I-LINK1019 Project, Spanish Ministry of Economy and Science, University of Cape Town Launching Grants Programme and National Research Foundation grant 99077 2016-2018, Ref. No. CSUR150628121624 and NRF Incentive Funding for Rated Researchers (IPRR), Ref. No. IFR170131220846. PKSD acknowledges financial support from the National Research Foundation, NRF South



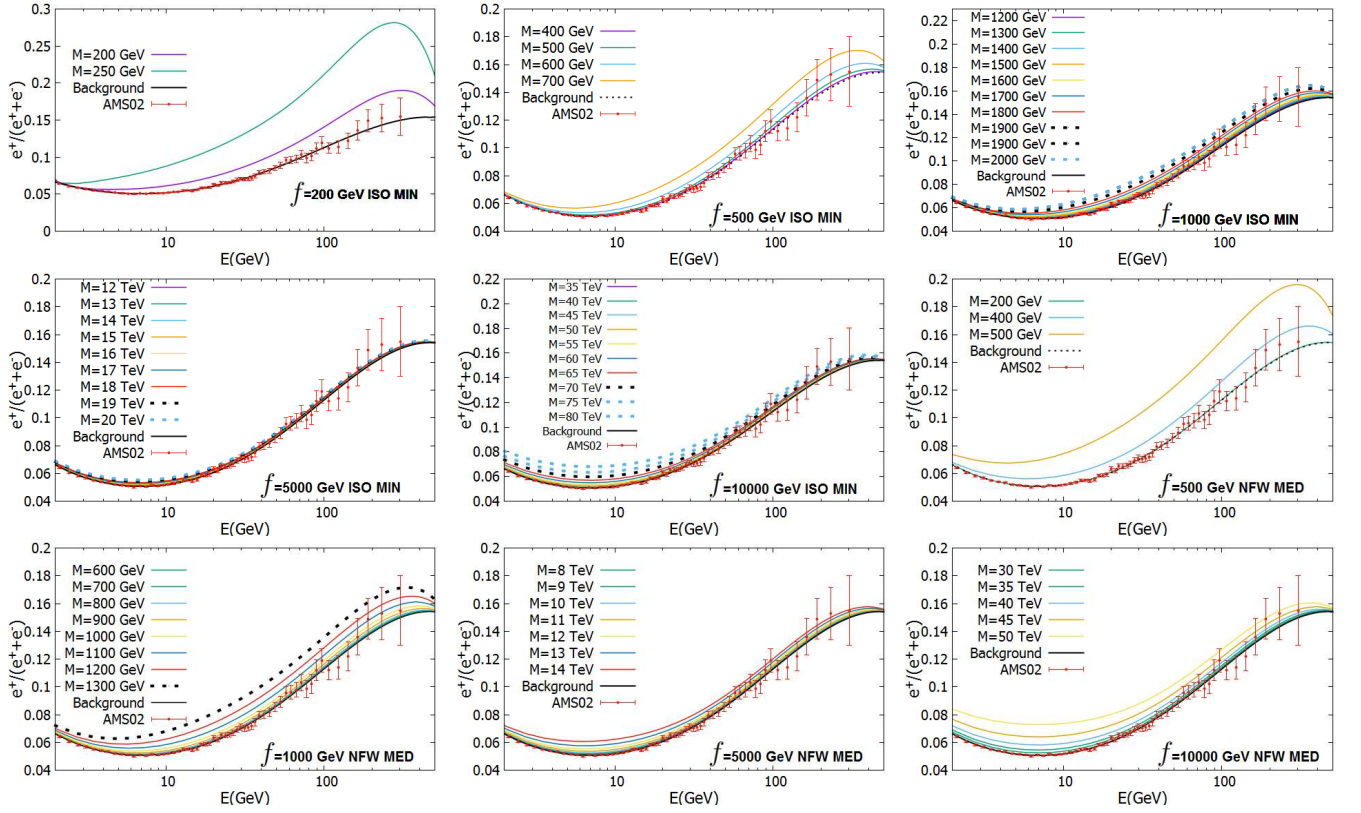


Figure 6: Positron fraction as obtained for branons in a theory of one extra dimension. The procedure to constrain the model of DM has consisted of discarding the masses for a tension of the brane unable to explain the AMS-02 experimental data within their error bars. For this, we have performed a  $\chi^2$  that helps us to build the exclusion map of Fig. 7 and 8. In addition, the effect of the tension suppressing the signal can be observed in the panels. For tensions greater than 15 TeV the signal is practically unobservable.

Africa. MMI acknowledges financial support from the University of Cape Town Doctoral Fellowships and the Erasmus+ Alliance4Universities Mobility Programme.

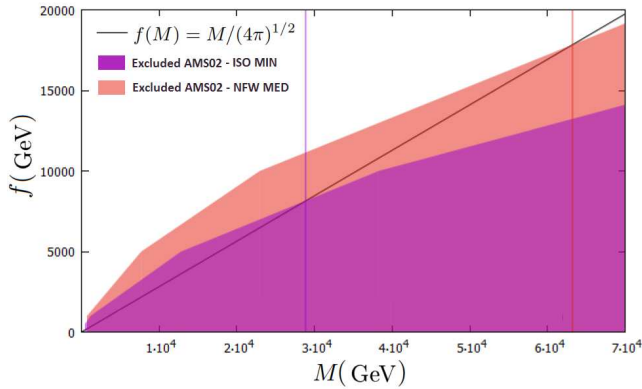


Figure 7: An exclusion diagram has been represented in this plot. The red one is for a model of halo pseudo Isothermal and in MIN diffusion. The pink one takes a NFW and the MED model. The line  $f(M) = M/(4\pi)^{1/2}$  represents an estimation of the limit of the validity of the effective theory for branons.

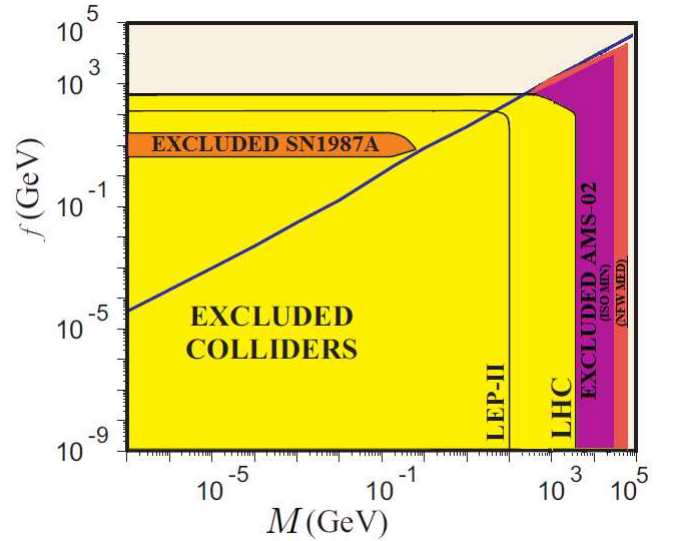


Figure 8: Combined exclusion plot taking some exclusion areas from ([103]), including LEP-II and LHC ([92, 104]), supernovae cooling ([94]) and the experimental exclusion from AMS-02 obtained in this paper. The purple zone is for a ISO, MIN model and the pink zone is for a NFW, MED model. The (blue) solid line is associated to the correct DM abundance of branons computed with the freeze-out mechanism.

- 
- [1] C. Pizzolotto [AMS-02 Collaboration], EPJ Web Conf. **121** (2016) 03006.
- [2] S. Caroff [AMS-02 Collaboration], arXiv:1612.09579 [astro-ph.HE].
- [3] M. Aguilar *et al.* [AMS Collaboration], Phys. Rev. Lett. **110** (2013) 141102.
- [4] O. Adriani *et al.* [PAMELA Collaboration], Nature **458** (2009) 607 [arXiv:0810.4995 [astro-ph]].
- [5] O. Adriani *et al.* [PAMELA Collaboration], Phys. Rev. Lett. **111** (2013) 081102 [arXiv:1308.0133 [astro-ph.HE]].
- [6] M. A. DuVernois *et al.*, Astrophys. J. **559** (2001) 296.
- [7] Ackermann, M., Ajello, M., Allafort, A., et al. 2012, Physical Review Letters, 108, 011103
- [8] M. Di Mauro, F. Donato, N. Fornengo, R. Lineros and A. Vittino, JCAP **1404** (2014) 006 [arXiv:1402.0321 [astro-ph.HE]].
- [9] P. F. Yin, Z. H. Yu, Q. Yuan and X. J. Bi, Phys. Rev. D **88** (2013) no.2, 023001 [arXiv:1304.4128 [astro-ph.HE]].
- [10] A. Erlykin and A. W. Wolfendale, Astropart. Phys. **49** (2013) 23 [arXiv:1308.4878 [astro-ph.HE]].
- [11] T. Delahaye, F. Donato, N. Fornengo, J. Lavalle, R. Lineros, P. Salati and R. Taillet, Astron. Astrophys. **501** (2009) 821 [arXiv:0809.5268 [astro-ph]].
- [12] H. Yuksel, M. D. Kistler and T. Stanev, Phys. Rev. Lett. **103** (2009) 051101 [arXiv:0810.2784 [astro-ph]].
- [13] Green, D. A. 2009, Bulletin of the Astronomical Society of India, 37, 45
- [14] Taylor, J. H., Manchester, R. N., & Lyne, A. G. 1993, APSJ, 88, 529
- [15] T. Delahaye, R. Lineros, F. Donato, N. Fornengo and P. Salati, Phys. Rev. D **77** (2008) 063527 [arXiv:0712.2312 [astro-ph]].
- [16] M. Grefe, J. Phys. Conf. Ser. **375** (2012) 012035 [arXiv:1111.7117 [hep-ph]].
- [17] L. Feng, R. Z. Yang, H. N. He, T. K. Dong, Y. Z. Fan and J. Chang, Phys. Lett. B **728** (2014) 250 [arXiv:1303.0530 [astro-ph.HE]].
- [18] A. Ibarra, A. S. Lamperstorfer and J. Silk, Phys. Rev. D **89** (2014) no.6, 063539 [arXiv:1309.2570 [hep-ph]].
- [19] Zwicky, F. 1933, Helvetica Physica Acta, 6, 110
- [20] Zwicky, F. 1937, *Astrophys. J.*, 86, 217
- [21] Clowe, D., Gonzalez, A., & Markevitch, M. 2004, *Astrophys. J.*, 604, 596
- [22] D. Clowe, M. Bradac, A. H. Gonzalez, M. Markevitch, S. W. Randall, C. Jones and D. Zaritsky, Astrophys. J. **648** (2006) L109 [astro-ph/0608407].
- [23] Rubin, V. C., & Ford, W. K., Jr. 1970, *Astrophys. J.*, 159, 379
- [24] Rubin, V. C., Ford, W. K., Jr., & Thonnard, N. 1980, *Astrophys. J.*, 238, 471
- [25] R. Massey, T. Kitching and J. Richard, Rept. Prog. Phys. **73** (2010) 086901 [arXiv:1001.1739 [astro-ph.CO]].
- [26] L. Anderson *et al.* [BOSS Collaboration], Mon. Not. Roy. Astron. Soc. **441** (2014) no.1, 24 [arXiv:1312.4877 [astro-ph.CO]].
- [27] E. W. Kolb, NATO Sci. Ser. C **534** (1999) 239
- [28] B. Audren, J. Lesgourgues, G. Mangano, P. D. Serpico and T. Tram, JCAP **1412** (2014) no.12, 028 [arXiv:1407.2418 [astro-ph.CO]].
- [29] R. J. Wilkinson, J. Lesgourgues and C. Boehm, JCAP **1404** (2014) 026 [arXiv:1309.7588 [astro-ph.CO]].
- [30] J. Miralda-Escude, Astrophys. J. **564** (2002) 60 [astro-ph/0002050].
- [31] J. Fan, A. Katz, L. Randall and M. Reece, Phys. Rev. Lett. **110** (2013) no.21, 211302 [arXiv:1303.3271 [hep-ph]].
- [32] Lacey, C. G., & Ostriker, J. P. 1985, *Astrophys. J.*, 299, 633
- [33] S. Tremaine and J. E. Gunn, Phys. Rev. Lett. **42** (1979) 407.
- [34] J. Conrad and O. Reimer, Nature Phys. **13** (2017) no.3, 224 [arXiv:1705.11165 [astro-ph.HE]].
- [35] E. A. Baltz, eConf C **040802** (2004) L002 [astro-ph/0412170].
- [36] J. A. R. Cembranos, A. Dobado and A. L. Maroto, Phys. Rev. Lett. **90**, 241301 (2003).
- [37] T. Kugo and K. Yoshioka, Nucl. Phys. B **594**, 301 (2001).
- [38] J. A. R. Cembranos, A. Dobado and A. L. Maroto, AIP Conf. Proc. **670**, 235 (2003); hep-ph/0402142; hep-ph/0406076; hep-ph/0411076; astro-ph/0411262.
- [39] J. A. R. Cembranos, A. Dobado and A. L. Maroto, Int. J. Mod. Phys. D **13**, 2275 (2004) [hep-ph/0405165]; astro-ph/0503622; astro-ph/0512569; astro-ph/0611911.
- [40] A. L. Maroto, Phys. Rev. D **69**, 043509 (2004); Phys. Rev. D **69**, 101304 (2004).
- [41] J. A. R. Cembranos *et al.*, 0708.0235 [hep-ph]; JCAP **0810**, 039 (2008)
- [42] R. Sundrum, Phys. Rev. D **59**, 085009 (1999);
- [43] M. Bando *et al.*, Phys. Rev. Lett. **83**, 3601 (1999);
- [44] A. Dobado and A. L. Maroto, Nucl. Phys. B **592**, 203 (2001);
- [45] J. A. R. Cembranos, A. Dobado and A. L. Maroto, Phys. Rev. D **65** 026005 (2002); hep-ph/0107155
- [46] J. Alcaraz *et al.*, Phys. Rev. D **67**, 075010 (2003);
- [47] J. A. R. Cembranos, A. Dobado and A. L. Maroto, Phys. Rev. D **70**, 096001 (2004)
- [48] J. A. R. Cembranos, A. de la Cruz-Dombriz, A. Dobado, R. A. Lineros and A. L. Maroto, Phys. Rev. D **83** (2011) 083507 [arXiv:1009.4936 [hep-ph]]; V. Gammaldi, J. A. R. Cembranos, A. de la Cruz-Dombriz, R. A. Lineros and A. L. Maroto, Phys. Procedia **61** (2015) 694 [arXiv:1404.2067 [hep-ph]]; JHEP **1309** (2013) 077 [arXiv:1305.2124 [hep-ph]].
- [49] M. Cirelli *et al.*, JCAP **1103** (2011) 051 Erratum: [JCAP **1210** (2012) E01] [arXiv:1012.4515 [hep-ph]].
- [50] N. Fornengo, R. Lineros, M. Regis and M. Taoso, Phys. Rev. Lett. **107** (2011) 271302 [arXiv:1108.0569 [hep-ph]].
- [51] N. Fornengo, R. A. Lineros, M. Regis and M. Taoso, JCAP **1201** (2012) 005 [arXiv:1110.4337 [astro-ph.GA]].
- [52] A. Natarajan, J. E. Aguirre, K. Spekkens and B. S. Mason, arXiv:1507.03589 [astro-ph.CO].
- [53] A. McDaniel, T. Jeltema, S. Profumo and E. Storm, arXiv:1705.09384 [astro-ph.HE].
- [54] J. A. R. Cembranos, A. de la Cruz-Dombriz, A. Dobado and A. L. Maroto, *23rd International Symposium on Lepton-Photon Conference*, arXiv:0708.0235 [astro-ph].

- [55] M. Ackermann *et al.* [Fermi-LAT Collaboration], Phys. Rev. D **86** (2012) 022002 [arXiv:1205.2739 [astro-ph.HE]].
- [56] P. Fermani [ANTARES Collaboration], Frascati Phys. Ser. **56** (2012) 244 [arXiv:1307.2402 [astro-ph.HE]].
- [57] M. Kachelriess, arXiv:0801.4376 [astro-ph].
- [58] A. P. Snodin, A. Shukurov, G. R. Sarson, P. J. Bushby and L. F. S. Rodrigues, Mon. Not. Roy. Astron. Soc. **457** (2016) no.4, 3975 doi:10.1093/mnras/stw217 [arXiv:1509.03766 [astro-ph.HE]].
- [59] J. Wu, arXiv:1205.5007 [astro-ph.HE].
- [60] A. W. Strong, I. V. Moskalenko and V. S. Ptuskin, Ann. Rev. Nucl. Part. Sci. **57** (2007) 285 doi:10.1146/annurev.nucl.57.090506.123011 [astro-ph/0701517].
- [61] Q. Yuan, S. J. Lin, K. Fang and X. J. Bi, Phys. Rev. D **95** (2017) no.8, 083007 doi:10.1103/PhysRevD.95.083007 [arXiv:1701.06149 [astro-ph.HE]].
- [62] L. O. Drury and A. W. Strong, PoS ICRC **2015** (2016) 483 [arXiv:1508.02675 [astro-ph.HE]].
- [63] L. O. Drury and A. W. Strong, Astron. Astrophys. **597** (2017) A117 doi:10.1051/0004-6361/201629526 [arXiv:1608.04227 [astro-ph.HE]].
- [64] S. Recchia, P. Blasi and G. Morlino, Mon. Not. Roy. Astron. Soc. **462** (2016) no.4, 4227 doi:10.1093/mnras/stw1966 [arXiv:1603.06746 [astro-ph.HE]].
- [65] C. L. Sarazin, Astrophys. J. **520** (1999) 529 doi:10.1086/307501 [astro-ph/9901061].
- [66] Rybicki, George B., and Alan P. Lightman. Radiative processes in astrophysics. John Wiley & Sons, 2008.
- [67] A. Thornbury and L. O. Drury, Mon. Not. Roy. Astron. Soc. **442** (2014) no.4, 3010 doi:10.1093/mnras/stu1080 [arXiv:1404.2104 [astro-ph.HE]].
- [68] F. Donato, D. Maurin, P. Salati, A. Barrau, G. Boudoul and R. Taillet, Astrophys. J. **563** (2001) 172 doi:10.1086/323684 [astro-ph/0103150].
- [69] E. Carquin, M. A. Diaz, G. A. Gomez-Vargas, B. Panes and N. Viaux, Phys. Dark Univ. **11** (2016) 1 doi:10.1016/j.dark.2015.10.002 [arXiv:1501.05932 [hep-ph]].
- [70] A. Ibarra, D. Tran and C. Weniger, Int. J. Mod. Phys. A **28** (2013) 1330040 [arXiv:1307.6434 [hep-ph]].
- [71] Salati, P., Donato, F., & Fornengo, N. 2010, Particle Dark Matter : Observations, Models and Searches, 521
- [72] J. A. R. Cembranos, A. Dobado and A. L. Maroto, Phys. Rev. Lett. **90** (2003) 241301 [hep-ph/0302041].
- [73] T. Kugo and K. Yoshioka, Nucl. Phys. B **594** (2001) 301 [hep-ph/9912496].
- [74] J. A. R. Cembranos, A. Dobado and A. L. Maroto, AIP Conf. Proc. **670** (2003) 235 [hep-ph/0301009].
- [75] J. A. R. Cembranos, A. Dobado and A. L. Maroto, hep-ph/0402142.
- [76] J. A. R. Cembranos, A. Dobado and A. L. Maroto, hep-ph/0406076.
- [77] J. A. R. Cembranos, A. Dobado and A. L. Maroto, hep-ph/0411076.
- [78] J. A. R. Cembranos, A. Dobado and A. L. Maroto, astro-ph/0411262.
- [79] J. A. R. Cembranos, A. Dobado and A. L. Maroto, Int. J. Mod. Phys. D **13** (2004) 2275 doi:10.1142/S0218271804006322 [hep-ph/0405165].
- [80] Cembranos, J. A. R., A. Dobado, and A. L. Maroto. "Dark matter from extra dimensions." arXiv preprint astro-ph/0503622 (2005).
- [81] J. A. R. Cembranos, A. Dobado, J. L. Feng, A. L. Maroto, A. Rajaraman and F. Takayama, astro-ph/0512569.
- [82] J. A. R. Cembranos, A. Dobado and A. L. Maroto, astro-ph/0611911.
- [83] A. L. Maroto, Phys. Rev. D **69** (2004) 043509 [hep-ph/0310272].
- [84] A. L. Maroto, Phys. Rev. D **69** (2004) 101304 [hep-ph/0402278].
- [85] J. A. R. Cembranos, A. de la Cruz-Dombriz, A. Dobado and A. L. Maroto, JCAP **0810** (2008) 039 [arXiv:0803.0694 [astro-ph]].
- [86] R. Sundrum, Phys. Rev. D **59** (1999) 085009 [hep-ph/9805471].
- [87] M. Bando, T. Kugo, T. Noguchi and K. Yoshioka, Phys. Rev. Lett. **83** (1999) 3601 [hep-ph/9906549].
- [88] A. Dobado and A. L. Maroto, Nucl. Phys. B **592** (2001) 203 [hep-ph/0007100].
- [89] J. A. R. Cembranos, A. Dobado and A. L. Maroto, Phys. Rev. D **65** (2002) 026005 [hep-ph/0106322].
- [90] J. A. R. Cembranos, A. Dobado and A. L. Maroto, hep-ph/0107155.
- [91] V. Gammaldi, J. A. R. Cembranos, A. de la Cruz-Dombriz and A. L. Maroto, AIP Conf. Proc. **1458** (2011) 411 [arXiv:1202.1707 [astro-ph.CO]].
- [92] J. Alcaraz, J. A. R. Cembranos, A. Dobado and A. L. Maroto, Phys. Rev. D **67** (2003) 075010 [hep-ph/0212269].
- [93] J. A. R. Cembranos, A. Dobado and A. L. Maroto, Phys. Rev. D **70** (2004) 096001 [hep-ph/0405286].
- [94] J. A. R. Cembranos, A. Dobado and A. L. Maroto, Phys. Rev. D **68** (2003) 103505 [hep-ph/0307062].
- [95] Achard, Pablo, et al. Physics Letters B 597.2 (2004): 119-130.
- [96] P. Creminelli and A. Strumia, Nucl. Phys. B **596** (2001) 125 [hep-ph/0007267].
- [97] J. A. R. Cembranos, A. Dobado and A. L. Maroto, Phys. Rev. D **73** (2006) 035008 [hep-ph/0510399].
- [98] M. Cirelli, G. Corcella, A. Hektor, G. Hütsi, M. Kadastik, P. Panci, M. Raidal, F. Sala, A. Strumia, arXiv 1012.4515, JCAP 1103 (2011) 051. Erratum: JCAP 1210 (2012) E01.
- [99] P. Ciafaloni, D. Comelli, A. Riotto, F. Sala, A. Strumia, A. Urbano, arXiv 1009.0224, JCAP 1103 (2011) 019, where the energy spectra have been computed including electroweak corrections.
- [100] D. Maurin, F. Melot and R. Taillet, Astron. Astrophys. **569** (2014) A32, doi:10.1051/0004-6361/201321344, [arXiv:1302.5525 [astro-ph.HE]].
- [101] M. Aguilar *et al.* [AMS Collaboration], Phys. Rev. Lett. **113** (2014) 121102.
- [102] M. Graziani, arXiv:1701.07305 [astro-ph.HE].
- [103] J. A. R. Cembranos and A. L. Maroto, Int. J. Mod. Phys. **31** (2016) no.14n15, 1630015 [arXiv:1602.07270 [hep-ph]].
- [104] P. Achard *et al.* [L3 Collaboration], Phys. Lett. B **597** (2004) 145 [hep-ex/0407017].